International Journal of Engineering and Technology Research
Vol. 1, No. 10, November 2013, PP: 178 -185, ISSN: 2327-0349 (Online)
Available online at www.ijeatr.org

Research article

The Structural and Thermodynamic Properties of Amorphous and Liquid Aluminum

T V Mung [1], P H Kien [2*], T V Ha [3] and H V Hue [4]

[1] *Vinh Phuc College, Phuc Yen,Vinh Phuc, Vietnam*
[2] *Department of Physics, Thai Nguyen University of Education, Luong Ngoc Quyen, Thai Nguyen, Vietnam*
[3] *College of Information Technology and Communication – TNU, Quyet Thang,Thai Nguyen, Vietnam*
[4] *Faculty of General Science, Ho Chi Minh City University of Food Industry, 140 Le Trong Tan, Ho Chi Minh, Vietnam*
** E-mail: phkien80@gmail.com*

ABSTRACT

Molecular dynamics (MD) simulation study based on the embedded atom method (EAM) potential is carried out to investigate the effect of temperature on the microstructure and properties of aluminum (Al). The microstructure and thermodynamic properties are analyzed through pair radial distribution function, energy per an atom, radius distribution of simplexes and the fraction of simplex types. Results show that the local structure of aluminum significantly depends on temperature. The simulation result also shows that the melting point of amorphous aluminum is about 940 K. The second peak of radial distribution function splits at temperature range lower than 200 K. The mean radius of simplexes increases with temperature. The fraction of simplex-6 reaches minimum value at about 180K and this is the origin of splitting of the second peak.

Keywords: Aluminum, molecular dynamics, embedded-atom method, rapid cooling, liquid and amorphous.

1. INTRODUCTION

The study of structural and dynamical processes related to atomic motions in liquid and amorphous (LAM) systems present an attractive research topic, both of theoretical and experimental origin. This being so, the extent of corresponding experimental knowledge about structural and microscopic processes in liquids and amorphous has continuously increased [1-6]. A liquid and amorphous metal can form either a non equilibrium phase, which is obtained by rapid quenching so that the nucleation of equilibrium phase is suppressed, or alternatively, an equilibrium phase, the crystal if the quenching process is slow [7-11]. The structure and thermodynamic of liquid and amorphous Al is intensively studied using different techniques such as atomic force microscopy, transmission electron microscopy, extended X-ray absorption fine-structure techniques and simulation method [6]. Those works have provided much information about the microstructure properties at atomic level. For example, authors in ref. [12] revealed the structure of the electric pulse (EP)-modified liquid aluminum tends to be loose and unordered with increasing temperature, which is similar to that of the unmodified structure. A local structure transformation occurs when EP is introduced (at 750^0 C). Ref [13]

showed that the calculated viscosities of Al from MD simulation were in agreement with the lower limit of the viscosity range. They found that the diffusion data agrees very well with the phenomenological Sutherland-Einstein model. Study in ref. [14] has used empirically modified Lennard-Jones-type potential indicating that the liquid and amorphous Al agrees with experimental data for all the metals studied. A. Sarka [15] found that a high pressure lends to strong crystallization tendency during cooling. Nevertheless, very few works concerning the microstructure and thermodynamics of LAM Al have been done yet. Therefore, it is worth to carring a simulation of LAM Al in order to compile a picture of structure and thermodynamics of LAM Al.
In the present work we reveal how the local structure of aluminum depends on temperature. Splitting of the second peak of radial distribution function at temperature range lower than 200 K could be analyzed by the fraction of simplex-6 type in metal materials. The melting point of amorphous aluminum has also been determined by the variation of the cohesive energy with temperature. The paper is organized as follows. After a brief introduction we describe in detail the simulation technique in section 2. The analyzing role of simplexes detected in LAM Al, estimation of melting temperature and determining specific heat are presented in section 3. Section 4 is devoted to the main conclusions.

2. CALCULATION METHOD

The MD simulation was carried out in sample cubic box with periodic boundary conditions for bulk Al containing 2013 atoms. The equations of motion of atom were numerically solved using the velocity version of Verlet algorithm. We use the Sutton-Chen EAM model which successfully reproduces liquid metals at different temperatures and pressures [3]. In accordance to this model the total energy is written as:

$$E_{total} = \sum_{i=1}^{N} E_i \tag{1}$$

Further

$$E_i = \frac{1}{2}\sum_{j\neq i}^{N} \Phi\left(r_{ij}\right) + F_i\left(\rho_i\right) \tag{2}$$

With

$$\rho_i = \sum_{j\neq i}^{N} \rho\left(\rho_{ij}\right) \tag{3}$$

Where N is number of atoms; r_{ij} is a distance between atoms i and j. The particular functions Φ, ρ_i and $F_i(\rho)$ are

$$\Phi\left(r_{ij}\right) = \varepsilon\left(\frac{a}{r_{ij}}\right)^n \tag{4}$$

$$\rho\left(r_{ij}\right) = \left(\frac{a}{r_{ij}}\right)^m \tag{5}$$

$$F_i\left(\rho_i\right) = -\varepsilon c\sum_{i=1}^{N}\sqrt{\rho_i} \tag{6}$$

Where ε is a parameter in energy unit, a is the lattice constant, c is a positive dimensionless parameter, m and n are integers [4]. These potential parameters taken from literature and some physical properties of LAM Al are given in Table 1 [5].

Table 1. The parameters of Sutton-Chen version of the EAM functions and some properties of Al; ρ is density of mass, r_0 is the distance of nearest neighbor atoms, T_m is melting temperature, R_{atom} is atom radius.

ε(eV)	a(Å)	c	m	n	ρ (g/cm^3)	T_m(K)	r_0(Å)	R_{atom}(Å)
3.3147	4.05	16.399	6	7	2.7	933.5	2.86	1.82

We first place 2013 atoms in a cubic box with periodic boundary condition. Then the melt equilibrated at 2000 K was obtained by relaxing the sample over 10^5 MD steps under constant temperature and ambient pressure. Here, the MD step is equal to 1.4×10^{-15} s. After that the melt is cooled down to difference temperatures ranging from 50 to 1600 K in order to construct the LAM Al models. Next, the final samples are obtained by relaxing

the above constructed models for a long time with 10^5 MD steps. Those obtained temperature models are used to study the structural and thermodynamic properties in LAM Al. The details of obtained results are discusses in section 3.

3. RESULTS AND DISCUSSION

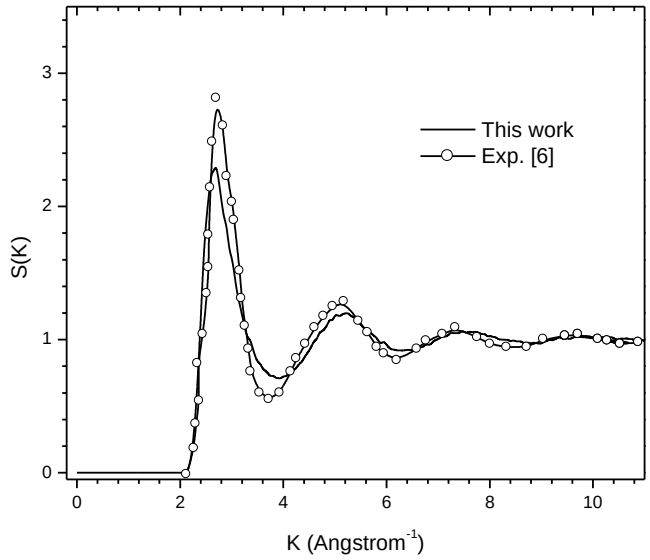

Fig. 1. The structure factor for Al obtained model and experiment data at 670 C.

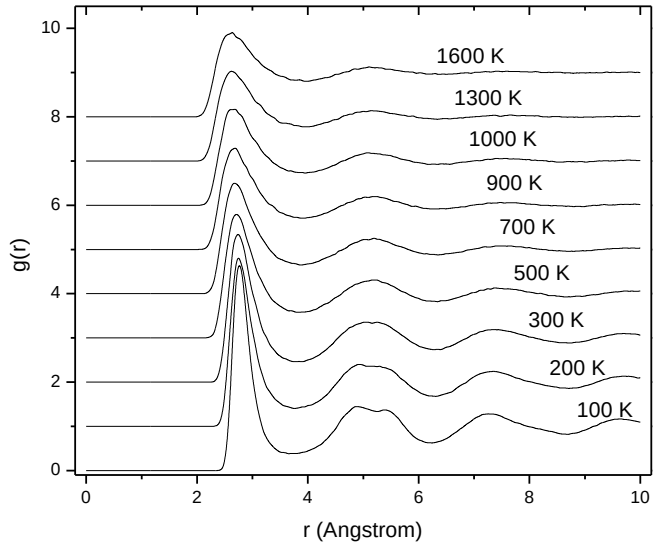

Fig. 2. The pair radial distribution functions for obtained amorphous and liquid Al models at different temperature.

The structure factor (SF) in LAM Al has been studied both by the neutron and x-ray diffraction techniques [2, 6]. Our simulation can be compared to these experiments and therefore allowed us to test the reliability of constructed models. As shown in Fig. 1, compared to experimental data in ref. [6], the SF is in good agreement with our simulation result. Therefore, our obtained models can be used for further study of the structure and thermodynamic properties of LAM Al. As shown in Fig. 2, the first peak intensities of the pair radial distribution functions (PRDF) curves increase and shift from left to right with decreasing temperature. The main characteristics of obtained models are listed in Table 2. One can see that the energy per atoms, the first peak position and the height of PRDF curves decrease, meanwhile the volume of model increases with increasing temperature. So it can be concluded that the nearest neighboring coordination is raised during solidification of Al. The PRDF *g(r)* plotted in Fig. 2 show a split of second peak at temperature range lower than 200 K, which is also observed by experimental researchers for Al and different amorphous materials [6,14].

It can be found that different methods are suggested to determine the melting temperature (T_m) which is observed widely of amorphous and liquid material. A few methods for the determination of T_m have been used in MD simulations [7, 10]. It has been known that the caloric curve method used in this study always gives a lower melting point than experimental data. For our MD simulation the temperature T_m can be determined via the intersection of a linear high temperature and low temperature extrapolation of the potential energy of the system as shown in Fig. 3 for the models at temperature range from 100 to 1600K. As show in Fig. 3, the melting temperature of Al is equal to about 940 K. This value is in good agreement with experimental data (943 K) in ref. [6]. Further, the specific heat (C_V) of LAM Al can be calculated by formula (7).

$$C_V = -\left(\frac{\partial E}{\partial T}\right)_V \qquad (7)$$

Where E is the energy per atom, T is temperature. From Fig. 3 data and equation (7) one can calculate specific heat, which is equal 0.15×10^{-3} eV/K for $T \le T_m$ and 0.11×10^{-3} eV/K for the case of $T > T_m$.

Table 2. The characteristics of LAM Al at difference temperatures; T is temperature, ε is averaged energy per atom, V is volume of model; r_{max} and $g(r_{max})$ are the position and the height of the first peak of the PRDF, respectively; n_S-4, n_S-5, n_S-6 and n_S-7 are the number of simplexes which has 4, 5, 6 and 7 atoms around, respectively; $N_{vacancy}$ is the number of found native vacancy in models.

Model	***T(K)***	***ε(eV)***	***V (nm^3)***	***r_{max}***	***$g(r_{max})$***	***n_S-4***	***n_S-5***	***n_S-6 ($\times10^{-1}$)***	***n_S-7 ($\times10^{-2}$)***	***$N_{vacancy}$***
M_1	50	-3.283	34.833	2.75	5.33	5.515	0.484	0.040	0	0.068
M_2	100	-3.278	34.718	2.75	4.69	5.510	0.504	0.368	0	0.109
M_3	150	-3.265	35.254	2.75	3.97	5.503	0.552	0.030	0	0.144
M_4	200	-3.263	35.232	2.75	3.86	5.519	0.519	0.298	0	0.245
M_5	250	-3.253	35.679	2.75	3.60	5.497	0.566	0.044	0	0.215
M_6	300	-3.246	35.679	2.75	3.71	5.440	0.624	0.462	0.099	0.514
M_7	400	-3.230	36.088	2.70	3.02	5.493	0.652	0.447	0.099	0.722
M_8	500	-3.215	36.546	2.70	2.81	5.462	0.708	0.621	0.000	1.070
M_9	600	-3.199	37.076	2.70	2.51	5.465	0.731	0.720	0.000	1.326
M_{10}	700	-3.185	37.623	2.70	2.49	5.466	0.769	0.576	0.348	1.605
M_{11}	800	-3.171	38.091	2.65	2.41	5.385	0.856	0.532	0.149	1.956
M_{12}	900	-3.157	38.574	2.65	2.31	5.426	0.859	0.576	0.546	2.224
M_{13}	1000	-3.148	39.016	2.65	2.15	5.443	0.852	0.710	0.646	2.420
M_{14}	1150	-3.130	39.629	2.65	2.13	5.440	0.857	0.825	0.745	2.698
M_{15}	1300	-3.113	40.325	2.60	2.03	5.362	0.994	0.825	0.497	3.112
M_{16}	1450	-3.095	41.206	2.60	1.98	5.384	0.942	0.949	1.093	3.303
M_{17}	1600	-3.083	41.678	2.60	1.87	5.410	0.926	1.098	1.397	3.407

International Journal of Engineering and Technology Research
Vol. 1, No. 10, November 2013, PP: 178 -185, ISSN: 2327-0349 (Online)
Available online at www.ijeatr.org

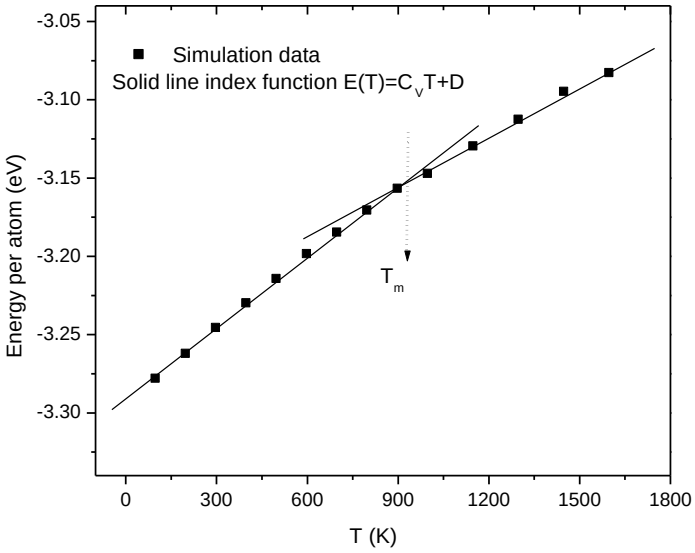

Fig. 3. Dependence of energy per an atom under temperature of LAM Al

Useful information about local structure can be inferred from simplex analysis. The simplex is defined as a set of four nearest neighboring atoms which form a tetrahedron. In addition, there is not any atom inside the circum-sphere (CS) of this tetrahedron (the vertices of the tetrahedron lie on the surface of CS). The simplex radius is denoted as the radius of CS. More detail about the method determining the simplexes can be found elsewhere [8]. The number of simplex-types in obtained models is listed in Table 2. One can see that the simplex-4 type per atom insignificantly changes under temperature. However, the number of simplex-5, -6 and -7 type per atom significantly increase with increasing temperature, i.e. the number of simplex-5, -6 and -7 per atom monotonically increase corresponding from 0.484×10^{-1}, 0.040×10^{-1} and 0 to 0.926×10^{-1}, 1.098×10^{-1} and 1.397×10^{-2}, respectively. Fig. 4 shows the distribution of simplex radius (DSR) for LAM Al. As can be seen the height of the main peak of DSR decreases and shifts to the larger position with increasing temperature, i.e. the height and location of main peak change from 1.95 per atom and 1.8 Å to 1.18 per atom and 2.1 Å when the temperature increases from 100 to 1600 K, respectively. Fig. 4 also shows that at high temperature, the DSR is spread wider than at low temperature. From above data analysis we can conclude that the lower the temperature of model is, the more homogeneous its structure is.

Now we turn to discuss the role of simplex for diffusion mechanism. As show in Fig. 4 the DSR is widely spread in the interval from 1.4 to 2.8 Å. It is worth to note that the shortest distance between two atoms in the bulk Al is 2.025 Å. Therefore, if one inserts an atom inside the simplex with radius bigger than 2.025 Å, then the distance between the inserting atom and any another atom is also bigger than 2.025 Å. It means that such simplex behaves like an "empty node" in liquid and amorphous matrix, where one atom is removed. This picture is similar to the case that if we remove one atom from the all crystal lattice, for instance Al crystalline, then a large simplex is created. The distance from this simplex to any atom is bigger than the shortest distance between two atoms in the Al crystalline lattice. This simplex is considered as vacancy in crystalline lattice. By analogy the simplex with radius bigger than 2.025 Å, can be considered as a “native vacancy” in LAM Al. Schematic illustration for determining the native vacancy in amorphous matrix is shown in Fig. 5. The native vacancy could play a role of vacancy but their concentration weakly depends on the temperature. This leads to that the activation energy for self-diffusion is mainly determined by migration part and not as sum of migration and formation energy. This property is observed experimentally for certain amorphous T-based (T is Fe, Co, Ni or Al) alloys where the activation energy is significantly lower than those of the crystalline counterpart [2, 8, 9]. Therefore it is interesting to determine the number of non-overlapping simplexes with radius bigger than 2.025 Å which determines the concentration of native vacancy. The result is presented in Table 2. It can be seen that the number per atom (N_{vacancy}) monotonically increasing with increasing the temperature, i.e. the number per atom increases from 0.068 to 3.407 with increasing temperature from 50 to 1600 K. Although the number of

native vacancy little influences on the main characteristics such as activation energy and the distribution of coordination number, however it characterizes the homogeneity in liquid and amorphous structure similar to the role of simplexes. Therefore, the lower the temperature, the more homogeneous its structure is. Combining with above results one can conclude that the diversity in LAM Al is caused mainly by the number of native vacancy (simplex with radial R > 2.025 Å).

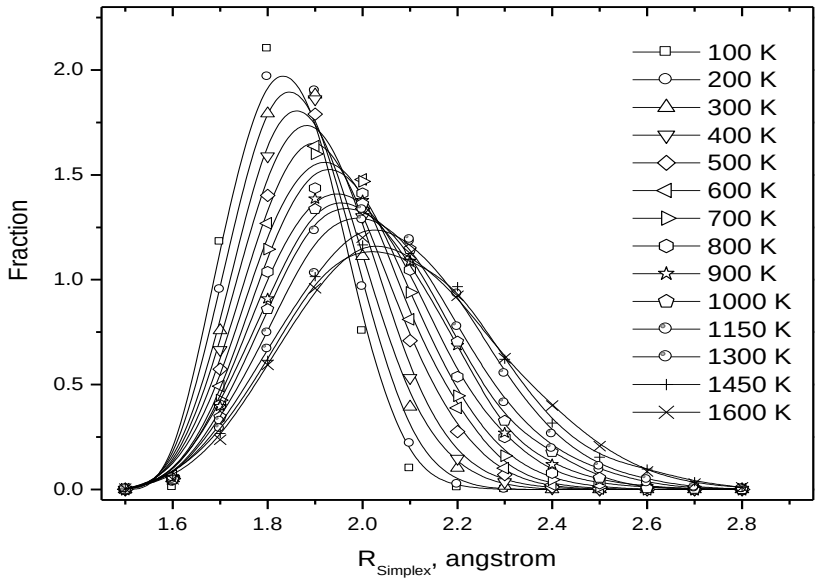

Fig. 4. The mean radius distribution of simplexes at different temperature

(a) (b)

Fig. 5. Schematic illustration of different simplex types: (a) Simplex-4 with smaller radius than 1.9 Å; (b) Simplex-7 with bigger radius than 2.05 Å which is called "native vacancy" in LAM Al. The white ball is CS, and the black ball is aluminum atom.

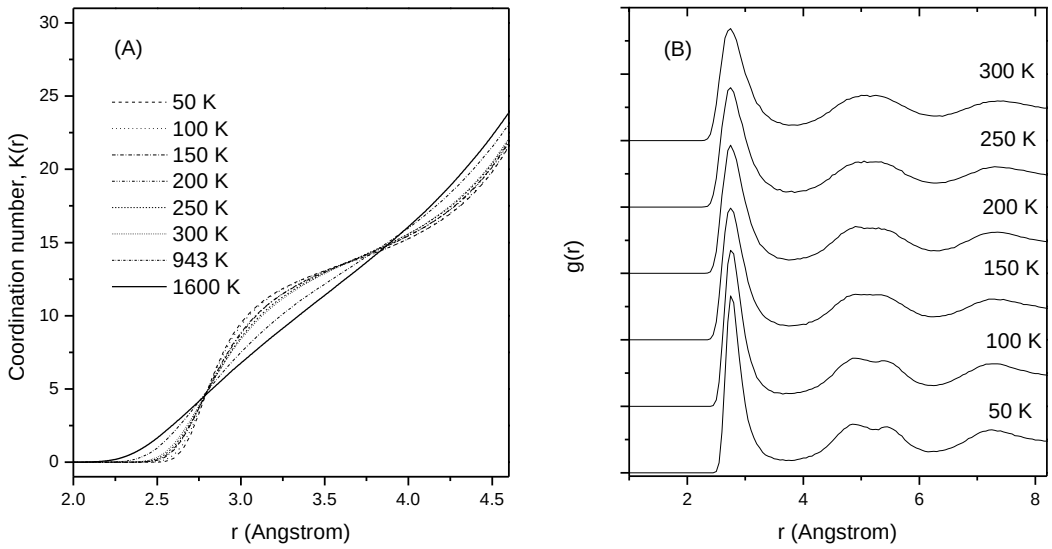

Fig. 6. Running coordination numbers (A) and splitting on the second peaks of the pair radial distribution functions (B) of some selected models at different temperatures.

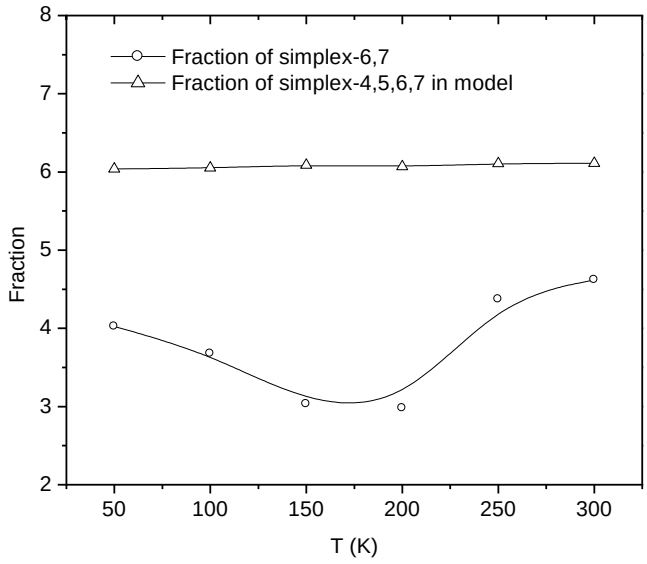

Fig. 7. Dependent fraction of simplex-6 and 7 and total of simplexes on temperature in LAM Al

Next, we turn to discuss the role of simplex for splitting of the second peak of RPDFs. Fig. 6 gives the running coordination numbers (RCN) and PRDFs of some different temperature models. As shown in Fig. 6A, at the temperature 50 K, the first coordination shell around the Al atom contains 13 Al atoms with the first minimum of PRDF of 3.45 Å. The RCN curves slightly changes in the temperature range 50-300 K. In contrast, in the temperature range 300-1600 K, the RCN curves significantly shifts to a lower first coordination shell with increasing temperature. On the other hand, it can see in Fig. 6B, at lower than 200 K the second peak starts splitting into two small peaks. The splitting is observed as two maximums at 4.9 and 5.5 Å at 50 K, those values are also found by previous experimental researches [6,14]. This splitting is often thought to be related to the

existence of an icosahedron and is defined as a common feature of amorphous material. Our MD simulation indicated that the splitting of the second peak is related to the simplex distribution in amorphous metals. The dependent number of simplex-6 and 7 and total of simplexes per atom under temperature of amorphous Al is plotted in Fig. 7 in the temperature range 50-300 K. As can be seen that the fraction of total simplexes of the model dose not depend temperature. However, the shape of fraction of simplex-6 and 7 shows a minimums position at 180 K. At below 180 K, the fraction of simplex-6 and 7 increases lead to the splitting of the second peak of PRDF being clearer. From above analysis we can conclude that the splitting of the second peak is only related the simplex-6 and 7 distributions.

4. CONCLUSION

In summary we employ molecular dynamic simulation with Sutton-Chen EAM to investigate the microstructure of LAM Al consisting 2013 atoms. Our study addresses the homogeneous structure at difference temperatures of LAM Al. The simulation result shows that calculated melting temperature of Al metal is in good agreement with experimental data. Further, the splitting of the second peak of the radial distribution function is believed to be related to the simplex-6 and 7 distributions. Moreover, the simulation results also reveal the role of the large simplexes or native vacancies for self-diffusion in amorphous metal matrix. Therefore we can hope that the investigated results of properties of simplexes may be applied in real materials.

ACKNOWLEDGEMENTS

We are grateful to Professor P K Hung for many enlightening discussions on the problems discussed here.

REFERENCES

[1] Ozgen S, Duruk E. Molecular dynamics simulation of solidification kinetics of aluminum using Sutton–Chen version of EAM. Mater. Lett.. 2004; 58:1071-1075.
[2] Lopez JM and Silbert M. Structural diffusion model calculations of the pair distribution function of aluminum: From the liquid to the amorphous phase. Solid State Communications. 1989;69:585-587.
[3] Sutton AP, Chen J. Long-range Finnis – Sinclair potentials. Philos. Mag. Lett., 1990;61:139-146.
[4] Sutton AP, Pethica JB, Rafii-Tabar H, Nieminen JA, Mechanical properties of metals at the nanometre scale, ln: Electron theory in alloy design, Editor(s): Pettifor, Cottrell, London, Institute of Materials, 1992.
[5] Kittel C. Introduction to Solid State Physics. Wiley, New York. 1986:42.
[6] Waseda Y. The structure of liquids, amorphous solids and solid fast ion conductors. Progress in Materials Science. 1981;26:1-122.
[7] Haile JM. Molecular Dynamics Simulation, Elementary Methods. Wiley, Canada. 1992;224.
[8] Hung PK, Kien PH. New model for tracer-diffusion in amorphous solid. Eur. Phys. J. B. 2010;78:119-125.
[9] Frank W, Horvath J and Kronmuller H. Diffusion mechanisms in amorphous alloys. Materials Science and Engineering. 1988;97:415-418.
[10] Nayak SK, Khanna SN, Rao BK and Jena P. Thermodynamics of small nickel clusters. Journal of Physics Condensed Matter. 1998;10:10853-10862.
[11] Solhjoo S, Simchi A and Aashuri H. Molecular dynamics simulation of melting, solidification and remelting processes of aluminum. Transaction of Mechanical Engineering. 2012;36:13-23.
[12] Jingang Qi, Jianzhong Wang,Lijia He,Zuofu Zhao,Huiling Du. An investigation for structure transformation in electric pulse modified liquid aluminum. Physica B. 2011;406:846-849.
[13] Cherne FJ, Deymier PA. Calculation of the transport properties of liquid aluminum with equilibrium and non-equilibrium molecular dynamics. Scripta materialia. 2001;45:985-991.
[14] Stepanyuk VS et al. The microstructure of liquid and amorphous aluminum. Journal of Non-Crystalline solids. 1992;151:169-174.
[15] Sarkar A, Barat P and Mukherjee P. Molecular dynamics simulation of rapid solidification of Aluminum under pressure. International Journal of Modern Physics B. 2008;22:2781-2785.